ACS OMEGA

http://pubs.acs.org/journal/acsodf

Article

Preparation of Lighting in the Dark and Photochromic Electrospun Glass Nanofiber-Reinforced Epoxy Nanocomposites Immobilized with Alkaline Earth Aluminates

Amal T. Mogharbel, Ahmad A. Alluhaybi, Awatif R. Z. Almotairy, Meshari M. Aljohani, Nashwa M. El-Metwaly,* and Rania Zaky*

Cite This: *ACS Omega* 2023, 8, 1683−1692

Read Online

ACCESS | Metrics & More | Article Recommendations

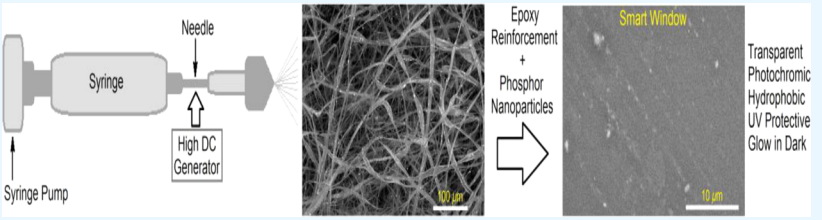

ABSTRACT: Alkaline earth aluminates (AEAs) as photoluminescent agents and silicon dioxide-based electrospun glass nanofibers with an average diameter of 150−450 nm as a roughening agent were prepared and applied to reinforce an epoxy resin toward the development of long-persistent photoluminescent and photochromic smart materials, such as smart windows and anticounterfeiting barcodes. With the physical immobilization of lanthanide-doped aluminate nanoparticles (NPs), a light-induced luminescent transparent glass@epoxy film was developed. The glass@epoxy samples were able to alter their color to green beneath ultraviolet rays and greenish-yellow in the dark, as explored by CIE Lab and luminescence spectral analyses. The morphology of the lanthanide-doped aluminate nanoparticles (43−98 nm) was examined by transmission electron microscopy (TEM). The morphologies and chemical composition of the luminescent glass@epoxy substrates were determined by different analytical techniques. The mechanical properties of the developed photoluminescent glass@epoxy substrates were inspected to show improved scratch resistance as compared to the AEA-free substrate. The photoluminescence spectra were measured to indicate the detection of two emission bands at 494 and 525 nm when excited at 365 nm. The photoluminescent glass@epoxy hybrids with lower AEA contents have showed fast reversibility of photochromism. On the other hand, the glass@epoxy substrates with higher phosphor contents underwent persistent luminescence. Results showed that the luminescent colorless glass@epoxy hybrids have enhanced superhydrophobicity and ultraviolet blocking.

1. INTRODUCTION

Rare earth oxides are a frequent component in the production of luminescent glasses. Glasses that emit light have been employed in a variety of lighting applications such as smart glass windows. Rare earth oxides are characterized by low cost, non-toxicity, photostability, and high-quality luminescence, making them ideal for use in smart windows.[1−4] Smart glass windows can be modified to display special effects such as photochromism, as well as ultraviolet and heat protection. Persistent photoluminescence is known as continuous emission in the near infrared, visible, and ultraviolet ranges after exposure to a light source followed by turning it off.[5,6] Modulating the duration and color of photoluminescence is a hot research topic in science. Thus, innovative displays, smart windows, and cutting-edge photonic devices are made possible. Both the hosting material and the doping compounds can affect the afterglow duration and color.[7−9] In recent years, studies focusing on the miniaturization of optical equipment have become more appealing. Lanthanide-activated nanomaterials are identified with remarkable photoluminescence effectiveness in a large range of electromagnetic spectra. Therefore, rare-earth-activated nano-scaled materials are employed in various optical tools such as light-emitting diodes. Smart commodities are able to undergo reversible and regulated changes in physical attributes when subjected to external stimuli such as poisonous compounds, light, and/or electric field.[10−12] As a result, protective devices have made use of a smart material ability to respond to potentially harmful

Received: November 25, 2022
Accepted: December 19, 2022
Published: December 28, 2022

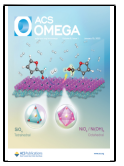

https://doi.org/10.1021/acsomega.2c07554
ACS Omega 2023, 8, 1683−1692

environmental stimulation, such as hazardous chemical agents and very high temperatures. Persistent emission permits a given material to continue releasing light long after the illumination source was turned off. The photochromic phenomenon has been known to employ ultraviolet light to induce colorimetric changes between two different optical states. A photochromic agent is able to regain its original optical condition when the illumination source is switched off.[13,14] Sensors, ophthalmic lenses, displays, and sunglasses are just some of the high-tech items that might benefit from the photochromic phenomenon. This advanced knowledge of light-induced chromic materials has shown to be highly useful in a variety of applications such as security barcodes, protection of trademark, UV shielding, military camouflage, and smart textiles.[15−18] Organic dyes make up the vast bulk of well-known photochromic agents. However, organic photochromic colorants have shown drawbacks such as expensive prices and low photostability. Owing to their steric hindrance, the immobilization of photochromic organic dyes in bulk materials reduces their photochromic activity because the photochromic response of these organic colorants to light is dependent on the molecule structure switching ability.[19,20] Thus, prolonged exposure to UV radiation can hasten the gradual loss of photostability of these organic dyes. On the other hand, inorganic photochromic dyestuffs are immune to steric hindrance because they do not rely on switching their molecular structure, providing improved photochromism with high photostability.[21] Alkaline earth aluminates (AEAs) have superior reversibility because of their remarkable photostability. Inorganic pigments with different emission colors include $CaMgSi_2O_6$:Eu^{2+},Dy^{3+} as the blue emitter, $SrAl_2O_4$:Eu^{2+},Dy^{3+} as the green emitter, and Y_2O_2S:Eu^{3+},Mg^{2+},Ti^{4+} as the red emitter.[22−24] This group of photochromic inorganic phosphors is notable for their high brightness, long-lasting emission (>10 h), and resilience to light, chemicals, and heat. Alkaline earth aluminates are advantageous since they are nontoxic and non-radioactive. Because of their photochromic and durable phosphorescence properties, the AEA has been favored for a wide variety of products.[25,26] It has been observed that the photochromic and long-lived phosphorescence characteristics of a certain bulk material change when the concentration of AEA changes. As a result, the physical inclusion of AEAs ($SrAl_2O_4$:Eu^{2+},Dy^{3+}) in a glass material introduces a new advance for the development of colorless smart glasses with persistent phosphorescence, fluorescence photochromism, robust surface, energy-saving character, and low cost.[27] Fluorescence can be defined as the material emission that stops instantly after turning the illumination source off. Phosphorescence and afterglow can be defined as the material emission that persists to emit light for a part of a second up to hours.[28,29] Fiber-reinforced polymeric composite materials have been developed by embedding fibers as fillers into the polymer bulk to improve the mechanical properties of those composite materials. The fiber-reinforced polymeric composite materials have been broadly used in various fields, such as satellites, automobiles, and aircrafts. Recently, inventive nanofibers have been an attractive research for the preparation of nanofiber-reinforced polymer nanocomposites.[30,31] This could be attributed to the high surface area of these nanofibers, leading to substantial enhancement of interfacial binding strength between the matrix and filler. The electrospinning technology has been able to offer a viable strategy for convenient preparation of ceramic, polymer, and carbon electrospun nanofibers. The preparation of silicon dioxide-based electrospun glass nanofibers has been reported to provide high mechanical strength and modulus toward nanofiber-reinforced polymer nanocomposites.[30−32]

Activation lanthanides ions, such as Eu^{2+}, are well-known photon emitters that are primarily triggered by ultraviolet light.[33] The unique optical, electrical, and magnetic properties of inorganic materials containing photoluminescent lanthanide activators have been reported. Because the 4f shells of lanthanide ions are only partly filled, they absorb and emit light at various energy levels when they are exposed to a light photon. The afterglow time of a photoluminescent agent, such as $SrAl_2O_4$:Eu^{2+},Dy^{3+}, is multiplied by a factor of 10 when co-doped with Eu^{2+} and Dy^{3+} at a certain ratio.[34] It was shown that Dy^{3+} can boost the luminous characteristics of Eu^{2+}-doped strontium aluminates and prolong the afterglow effect for more than 15 h. The inclusion of rare-earth ions in various kinds of glasses for potential optical electronic uses has been reported. The feasibility of obtaining luminous glass by doping host glass with lanthanide ions has been the subject of various recent research studies.[35] AEAs (MAl_2O_4; M = Sr, Ca, and Ba) are the most investigated luminous agents with persistent emission characteristics. The afterglow effect can be controlled by varying the proportion of AEAs in the hosting material. High quantum yield, chemically stable, safe, extended afterglow duration, and brilliant pure colors are only some of the intriguing luminescence characteristics offered by strontium aluminates doped with rare earth phosphors.[36]

Efforts to reduce energy consumption in buildings have motivated researchers to create more transparent materials with high light transmittance. The use of glass has allowed for the construction of efficient light-transmitting windows. However, long-persistent photoluminescent, photochromic, and energy-saving smart windows have been presented in a limited research.[37−39] In this context, the present study aims to develop a straightforward method for producing colorless glass@epoxy substrates with UV protection, long-lasting phosphorescence, photochromism, and hydrophobic activity. Photoluminescent glass@epoxy hybrids were developed using the electrospinning technology by immobilizing AEANPs throughout the glass@epoxy matrix. The morphology of AEA nanoparticles was investigated by TEM, whereas X-ray fluorescence (XRF), scanning electron microscope (SEM), and energy-dispersive X-ray (EDX) were applied to analyze the glass@epoxy morphology. The luminescence spectra were explored to analyze the optical properties of the glass@epoxy samples. The color screening findings from the CIE Lab on the colorless photoluminescent glass showed that under UV irradiation supply, the glass@epoxy substrate changed color to green. It was found that when the phosphor level in the glass@epoxy substrate increased, the scratch resistance of AEANP-embedded glass@epoxy substrates also increased. Better superhydrophobic properties were shown by analyzing the static contact angle. The current luminescent glass@epoxy hybrids are also photostable, providing smart windows with transparent photoluminescence properties for many potential applications such as safety warning, anti-counterfeiting, and soft lighting.

2. EXPERIMENTAL SECTION

2.1. Materials. 3-Aminopropyl triethoxysilane (APTES), polyvinyl pyrrolidone (PVP), tetraethylorthosilicate (TEOS), and 3-glycidoxypropyltrimethoxysilane (GPTMS) were ob-

https://doi.org/10.1021/acsomega.2c07554
ACS Omega 2023, 8, 1683−1692

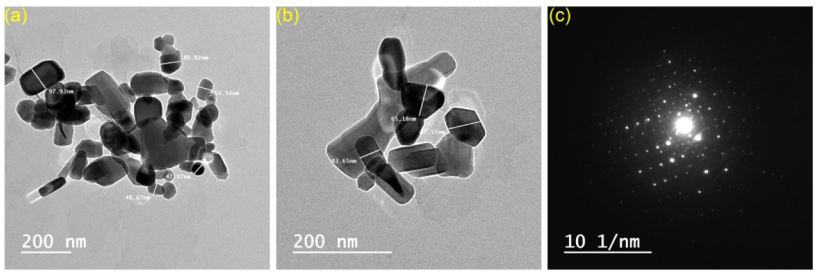

Figure 1. TEM histograms (a,b) and diffraction pattern (c) of AEANPs.

tained from Sigma-Aldrich (Egypt). Both the epoxy resin (SC-15A) and hardener (SC-15B) were obtained from Chemicals for Modern Building International (Egypt). The raw materials employed in the synthesis of AEAs include Eu_2O_3, Al_2O_3, Dy_2O_3, H_3BO_3, and $SrCO_3$ which were obtained from Merck (Egypt).

2.2. Preparation of AEANPs. The high-temperature solid-state technology[8,33] was applied to produce the AEA phosphor. In this procedure, 300 mL of absolute ethanol was combined with 0.2 mol of Al_2O_3, 0.002 mol of Eu_2O_3, 0.02 mol of H_3BO_3, 0.1 mol of $SrCO_3$, and 0.001 mol of Dy_2O_3. The mixture was then ultrasonically treated for 60 min at 35 kHz, dried for 22 h at 90 °C, and milled for 3 h. For 3 h, the generated residue was exposed to sintering at 1300 °C. The AEA nanoparticles were created by exposing the supplied phosphor microparticles to the top-down procedure.[40] The AEA microparticles (10 g) were inserted into a stainless-steel ball milling tube of 20 cm diameter located on a vibrating disc. The AEA powder in the tube was blasted with a ball mill made of silicon carbide (SiC) for 22 h to introduce AEANPs.

2.3. Electrospinning and Silanization. According to previously reported procedures,[31] the electrospun glass nanofibers were prepared by utilizing the spin dope composed of TEOS (13% w/w) and PVP (13% w/w) in mixed solvents of DMSO/DMF (1/2) followed by pyrolysis at 800 °C. The provided electrospun glass nanofibers were dispersed in water (5% w/w) and homogenized for 10 min. The silanization process was then performed by the immersion of the electrospun glass nanofibers in an ethanolic solution of silane (15% w/w), followed by heating to 50 °C and stirring for an hour at 125 rpm. The mixture was homogenized in ethanol for 10 min followed by rinsing with ethanol. The provided nanofibers were desiccated under vacuum.

2.4. Preparation of Photoluminescent Glass@epoxy. The electrospun glass nanofibers (1% w/w) were added to epoxy resin, exposed to stirring at 60 °C for 12 h at 125 rpm, and then homogenized for 30 min to assure homogeneous dispersion of the glass nanofibers. The phosphor nanoparticles (AEANPs) were added to the aforementioned solution at various concentrations, including 0.5, 1, 2, 4, 6, 8, 10, and 12% w/w. The resulting nanocomposites were denoted as AEA_0, AEA_1, AEA_2, AEA_3, AEA_4, AEA_5, AEA_6, AEA_7, and AEA_8. The mixture was exposed to stirring for 30 min at 125 rpm and then homogenized for 15 min. The hardener (30% w/w) was then added to the abovementioned mixture. The mixture was exposed to deaeration, added into an aluminum mold, subjected to curing at 60 °C for 2 h, and then cured at 110 °C for 5 h to provide a composite panel with a length of 200 mm, a width of 200 mm, and a thickness of 5 mm.

2.5. Methods. *2.5.1. Topographical Properties.* JEOL 1230 transmission electron microscopy (Jeol Instruments, Tokyo, Japan) was used to inspect the morphology of the AEA nanoparticles. A solution of AEANPs in CH_3CN was exposed to ultrasonication (35 kHz) for 10 min and dropped into a copper grid for TEM investigation. SEM Quanta FEG-250 (Czech Republic) was used to analyze the morphologies of the luminous glass@epoxy substrates. The elements of the luminous glass@epoxy substrates were determined using the TEAM-EDX setup coupled with SEM. The elemental composition of the glass@epoxy substrate was also analyzed using Axios sequential XRF (Panaco, Netherlands).

2.5.2. Hydrophobicity Screening. The contact angle was analyzed using OCA 15 EC (Dataphysics, Stuttgart, Germany).[41]

2.5.3. Mechanical Properties. Scratch resistance[42] and tensile strength[43] of the AEANP-embedded glass@epoxy nanocomposites were evaluated using the HB scratching pencil and Shimadzu ASTM D638M (Japan), respectively.

2.5.4. Photoluminescence Analysis. The photoluminescence spectra were analyzed using a JASCO FP-8300 (Japan). Phosphorescence accessory tools were applied to measure the photoluminescence decay and lifetime of the prepared glass@epoxy substrates. It took 15 min of UV excitation to obtain an accurate reading on the decay time. Results were presented in total darkness after shielding the glass@epoxy sample from the UV light source.

2.5.5. Ultraviolet Shielding. Samples of the luminous glass@epoxy hybrid were evaluated for their ability to block the ultraviolet rays using the ultraviolet protection factor (UPF).[44] An AATCC 183 2010 UVA standard protocol was followed to determine the UPF using a UV−vis spectrometer.

2.5.6. Reversibility Assessment. According to previous procedures,[34] the photoluminescent glass@epoxy sample was exposed to ultraviolet light for 5 min. Then, the glass@epoxy was stored in a dark wooden box for 60 min to regain its origin form. The fluorescence spectra were determined before and after UV illumination over many cycles.

2.5.7. Colorimetric Screening. Before and after illumination with UV, the glass@epoxy substrates were put through a colorimetric assessment by UltraScanPro (HunterLab; USA), which measured both the colorimetric strength (K/S) and CIE Lab parameters. The CIE Lab, standing for the French phrase "Commission Internationale de L'éclairage", has been recognized as the world foremost authority on color theory, lighting, and visual perception. Colors are described numerically in three-dimensional space using the CIE Lab system.[21] The Canon A710IS was employed to take pictures of the glowing glass@epoxy substrate both before and after being exposed to ultraviolet light.

https://doi.org/10.1021/acsomega.2c07554
ACS Omega 2023, 8, 1683−1692

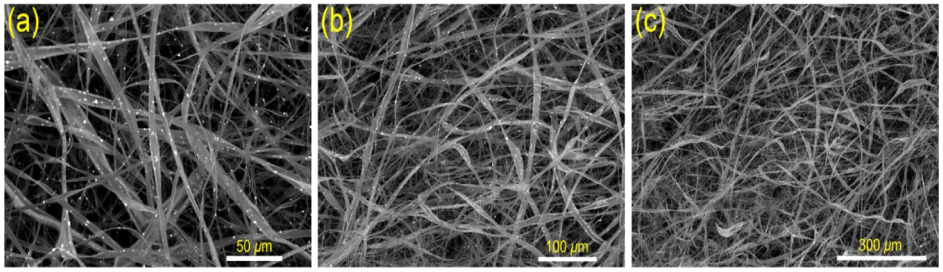

Figure 2. SEM histograms of glass fibers at different magnifications, 50 (a), 100 (b), and 300 μm (c).

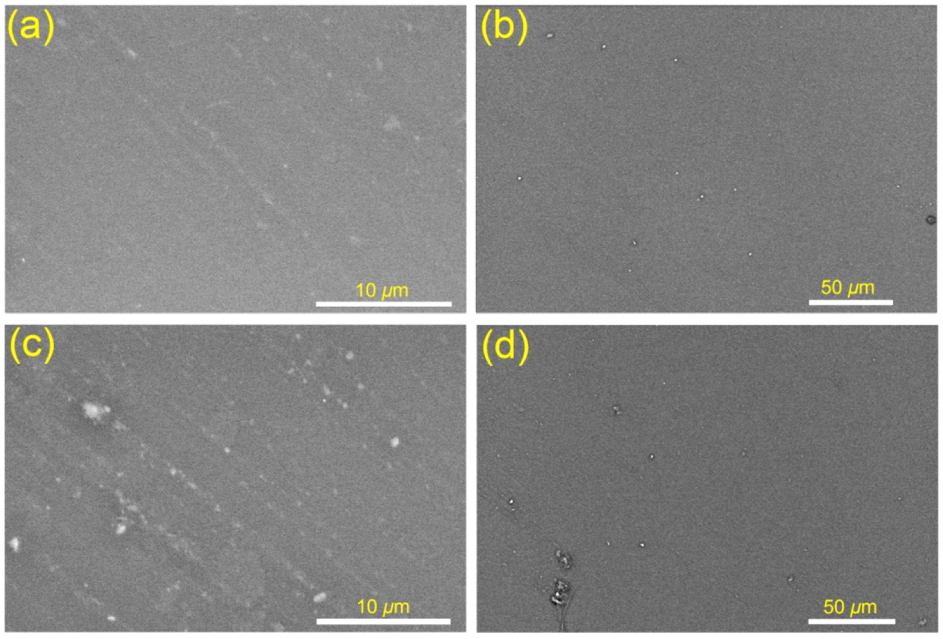

Figure 3. SEM histograms of AEANP-containing glass@epoxy substrates, AEA_0 (a,b) and AEA_6 (c,d).

Table 1. Elemental Contents (wt %) of AEANP-free and AEANP-Containing Glass@epoxy Nanocomposites as Monitored by EDS at Three Sites (S_1, S_2, and S_3) on Their Surfaces

glass@epoxy		Si	C	O	Al	Sr	Eu	Dy
AEA_0	S_1	17.10	45.79	37.20	0	0	0	0
	S_2	17.06	45.35	37.64	0	0	0	0
	S_3	17.18	45.57	37.32	0	0	0	0
AEA_1	S_1	14.31	43.73	38.87	1.62	1.11	0.30	0.16
	S_2	14.41	43.43	38.87	1.77	1.09	0.36	0.17
	S_3	14.81	43.42	38.51	1.67	1.25	0.23	0.13
AEA_3	S_1	13.15	42.62	39.44	3.66	2.14	0.61	0.42
	S_2	13.81	42.30	39.06	3.70	2.04	0.67	0.43
	S_3	13.49	42.38	39.16	3.97	2.15	0.58	0.36
AEA_6	S_1	7.32	41.08	40.28	6.55	3.29	0.90	0.66
	S_2	7.12	41.21	40.41	6.43	3.32	0.96	0.67
	S_3	7.01	41.00	40.20	6.78	3.52	0.96	0.54
AEA_8	S_1	4.15	41.24	41.31	7.24	4.18	1.21	0.72
	S_2	4.31	40.68	41.05	7.76	4.32	1.18	0.70
	S_3	4.11	41.00	41.14	7.37	4.55	1.05	0.79

3. RESULTS AND DISCUSSION

3.1. Preparation of Smart Windows. The AEA micropowder was synthesized by the high-temperature solid-state process,[33] and then, the produced AEA microparticles were subjected to the top-down method[40] to afford AEA nanoparticles. Using TEM, we were able to determine that AEANPs have a diameter of 43−98 nm (Figure 1). The ability of nanoscaled particles to maintain a particular matrix transparency is crucial.[45] Thus, the AEANPs were used to keep the glass@epoxy matrix transparent. The glass@epoxy hybrids were prepared at various concentrations of AEANPs. The electrospun glass nanofibers were prepared according to previously reported procedures.[31] The provided electrospun glass nanofibers and epoxy resin were mixed with different concentrations

https://doi.org/10.1021/acsomega.2c07554
ACS Omega 2023, 8, 1683−1692

of AEANPs. The electrospinning technique results in very uniform and versatile final products.[30−32] For a wide range of applications, including photochromic smart windows, directional signs, photonic products, soft indoor and outdoor lighting, and anti-counterfeiting materials, the current photochromic, superhydrophobic, and persistent phosphorescent and ultraviolet protective glass@epoxy substrates have been shown to be feasible for large-scale production.

3.2. Morphology Features. The topographical properties of the electrospun glass nanofibers and the glowing glass@epoxy substrates are shown in Figures 2 and 3. Table 1 displays the results of EDX analysis of the elemental compositions (wt %) of the glass@epoxy nanocomposites at three distinct surface sites (S_1, S_2, and S_3). There were relatively slight modifications to the surface morphology of the glass@epoxy substrates when the ratio of AEANPs was increased. The phosphor particles were found to be completely embedded into the glass@epoxy matrix, since no particles were found on the surfaces of the investigated glass@epoxy substrates. The developed electrospun glass nanofibers were studied by SEM to indicate diameters in the range of 150−450 nm, as shown in Figure 2.

Alkaline earth aluminate phosphor elements were confirmed by EDXA analysis. To determine the elemental contents of the manufactured glass@epoxy substrates, EDS analysis of the glass@epoxy surface was conducted at three different locations. The results showed that the phosphor particles were evenly distributed across the sample matrix, as evidenced by nearly identical elemental ratios at each of the three analyzed points. EDS examination revealed the presence of several elemental components, as indicated in Table 1. Elements such as strontium, aluminum, dysprosium, and europium were detected owing to the use of AEANPs, joining oxygen, carbon, and silicon as the main components in the glass@epoxy elemental composition. As a result of the low amounts of AEANPs used throughout the glass@epoxy manufacturing procedure, the elements such as strontium, aluminum, dysprosium, and europium were detected at low amounts. On the other hand, the elements such as oxygen, carbon, and silicon were detected at high amounts due to the presence of glass@epoxy as a bulk material in the manufacturing procedure.

As shown in Table 2, XRF analysis was also utilized to establish the chemical contents of the glowing glass@epoxy substrates. The EDXA technique allows for a more precise examination of a substance elemental composition. Elements present at concentrations of more than 10^3 g/kg can be detected by XRF.[46] Therefore, XRF offers an analytical approach for partial elemental identification of a certain substance. In the glass@epoxy substrates, XRF detected just the presence of aluminum and strontium. However, the traces of Eu and Dy were undetectable due to their minute quantities. The ratios of elements in both AEAs and luminous glass@epoxy substrates were found to be about the same ratios, as determined by EDX and XRF analysis.

Table 2. Elemental Contents of (wt %) of AEANP-free and AEANP-Containing Glass@epoxy Hybrids as Monitored by XRF

		content (wt %)			
element	oxide	AEA_1	AEA_3	AEA_6	AEA_8
Si	SiO_2	96.75	91.21	86.32	80.54
Sr	SrO	0.86	3.00	4.62	7.11
Al	Al_2O_3	2.39	5.79	9.06	12.35

3.3. Photoluminescence Spectral Analysis. Better visual perception of colorimetric transition to green requires a transparent background of a glass@epoxy substrate.[25] There was rapid and reversible photochromism monitored in the phosphor-infused glass@epoxy hybrid. The glass@epoxy with AEANP ratios comparable to or less than 1% were demonstrated to be instantaneously reversible to identify fluorescence emission. The samples of glass@epoxy with AEANP ratios greater than 1% continued to emit light when placed in darkness, demonstrating delayed reversibility, which is a property indicative of long-lasting phosphorescence emission. The excitation spectra showing the effect of phosphor concentration on the produced glass@epoxy hybrid composites are displayed in Figure 4. A time-reliant effect was observed between the time period of UV illumination (50−250 s) and the strength of the emission band. The luminescence spectra against the irradiation time for AEA_6 are shown in Figure 5. After being excited at 365 nm, the emission band was found to be at 525 nm. As the irradiation period increased, the strength of the emission intensity band increased. The glass@epoxy hybrid held the phosphor pigment nanoparticles as a

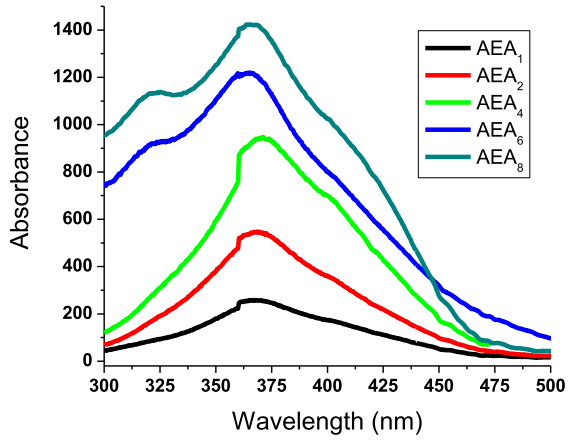

Figure 4. Excitation spectra of AEANP-containing glass@epoxy samples at 525 nm.

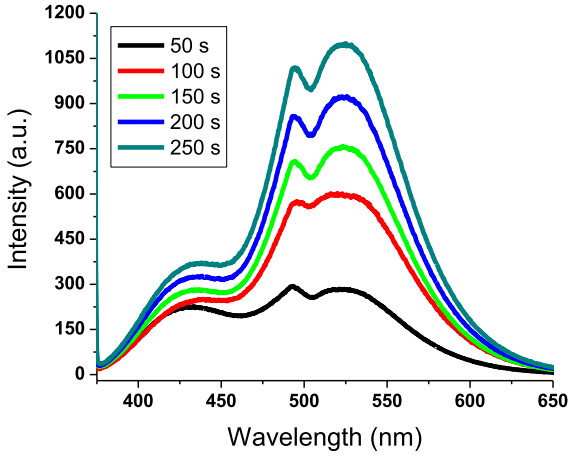

Figure 5. Emission spectra of AEA_6 as a function of increasing the period of the UV illumination (50−250 s).

https://doi.org/10.1021/acsomega.2c07554
ACS Omega 2023, 8, 1683−1692

colorless trapping medium. The inclusion of AEANPs strengthened the links between the glass@epoxy polymeric strands either by physically entrapping the AEA particles within the glass@epoxy bulk or by forming coordinative interactions between the positive Al(III) ions in the structure of AEAs and the glass@epoxy oxygen.[25,27]

The $4f \leftrightarrow 5d$ transition of Eu(II) was reported to emit green (525 nm) and blue (494 nm) lights. Two strontium sites in the $SrAl_2O_4$ crystal are accountable for these emission bands. However, the blue intensity is greatly diminished by the ambient thermal quenching.[33,34] Consequently, the greenish color emission was the only one detected. Because of this, we can conclude that the photoluminescence spectra were only impacted by the emissions generated by Eu(II) and not Eu(III). The decaying time demonstrates second-order exponential of the glass@epoxy substrate light over time. The decay curve decreased quickly at first and then slowed down over time.

3.4. Photochromic Analysis. The phosphor nanoparticles were mixed with the glass@epoxy hybrid to introduce a transparent smart window. To examine the photochromism of the manufactured glass@epoxy substrates, photographic images of AEA_6 were captured in both visible daylight and UV irradiation. There were significant vivid green emissions detected in UV; however, no traces were visible in daytime light. Photochromism, which can be triggered by exposure to ultraviolet light, has been put to use in a variety of anti-counterfeiting applications such as packaging. As a result, the present method can be used with any product that follows a common anticounterfeiting pattern. Gaskets were made out of the current glass@epoxy hybrid by cutting the pattern in a rectangular shape. The utilized gasket is transparent under daytime light but turns into a detectable green color when exposed to ultraviolet light, making it impossible to replicate. The present method can be considered as a competent technique due to its success in creating a wide variety of anticounterfeiting products for a better market. The optical transparency was tested to ensure the claimed clarity of the prepared glass@epoxy substrates. As the concentration of AEANPs in the glass@epoxy bulk increased, the optical transmittance slightly decreased. The transmission through AEA_1 was 93%, whereas the transmission through AEA_8 was 88%. The AEA_1 and AEA_8 samples seemed transparent in daytime light, revealing a greenish hue under ultraviolet light. The current photoluminescent colorless glass@epoxy hybrid composites are colorless under daylight, making it simpler to develop anti-counterfeiting fingerprints to avoid forgery of marketable products. The $4f^6 5D^1 \leftrightarrow 4f^7$ transition of Eu^{2+} is thought to be accountable for the emission of the AEA phosphor.[21] Since neither Eu^{3+} nor Dy^{3+} displayed any clearly distinguishable emission peaks, it was determined that Eu^{3+} had been exchanged for Eu^{2+}. It was also determined that the role of Dy^{3+} is to cause the development of traps that can release light in darkness, enabling Eu^{2+} to return to its ground state. For the photochromism and persistent luminescence of materials, reversibility is necessary to accomplish durability and photostability. Figure 6 shows the results of tests conducted to verify that AEA_6 has retained high reversibility without wearing down over a series of coloration and decoloration cycles when exposed to UV light and visible light, respectively.

3.5. Color Screening. The photoinduced chromic properties of the prepared glass@epoxy hybrid composites are summarized in Table 3. The glass@epoxy substrates from

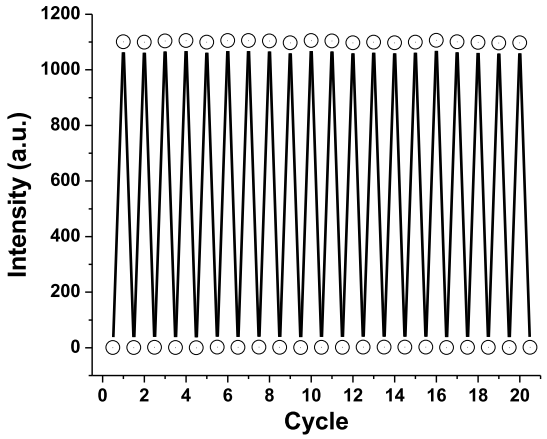

Figure 6. Reversibility of AEA_6 (525 nm) beneath ultraviolet and visible lights.

AEA_0 to AEA_6 exhibited a transparent appearance. However, the glasses from AEA_7 to AEA_8, which included more of the phosphor nanoparticles, appeared slightly white. Only if the AEANPs are uniformly distributed in the glass@epoxy bulk, the glass@epoxy substrates containing phosphor can be assured to have a transparent appearance even at contents of the phosphor nanoparticles. Nanomaterials have shown a remarkable ability to maintain a material transparency.[45,47] The colorless glass@epoxy substrates with low contents of phosphor nanoparticles (AEA_1 through AEA_2) showed a brilliant green fluorescence emission upon exposure to UV light. Green phosphorescence emission was detected when the glass@epoxy hybrid composites with high contents of phosphor nanoparticles (AEA_3 through AEA_8) were exposed to UV light, demonstrating greenish-yellow color in the dark. In response to UV light, the glass@epoxy hybrid became progressively greener as the AEANP concentration was increased. Under daylight, the colorimetric strength value slightly shifted, while the phosphor ratio was increased from AEA_0 to AEA_6. A considerable increase in the K/S was observed to designate a white shade when the phosphor ratio was increased from AEA_7 to AEA_8. When exposed to UV light, increasing the AEA nanoparticles in the glass@epoxy bulk from AEA_1 to AEA_8 resulted in increasing the K/S value. Because a green emission is produced under UV in contrast to the transparent appearance monitored in visible daytime, the K/S values were higher in UV than for the corresponding unirradiated glass@epoxy substrates. Changes in the CIE Lab for the AEANP-free glass@epoxy (AEA_0) were negligible both in visible and ultraviolet lights. In contrast, the phosphor-containing glass@epoxy substrates showed a broad range of values for the CIE Lab parameters. As the phosphor ratio was increased, the light transmission slightly dropped, causing L^* to slightly decrease in daylight. When the AEANP ratio was increased, it was shown that L^* decreased significantly under the UV device, suggesting an improvement in the greener shade. The $-a^*$ and $+b^*$ parameters showed low magnitudes with very minimal fluctuations with increasing AEANP ratio in daylight. When the AEANP ratio was increased, the magnitudes of $-a^*$ and $+b^*$ were shown to increase and decrease, respectively, beneath ultraviolet light. Turning off the UV instrument revealed that the luminous glass@epoxy hybrid composites with lower amounts of phosphor nanoparticles (AEA_1 and AEA_2) immediately returned to their transparent

https://doi.org/10.1021/acsomega.2c07554
ACS Omega 2023, 8, 1683−1692

Table 3. Color Screening of AEANP-free and AEANP-Containing Glass@epoxy Below Visible Light (VL), and UV Radiation

	K/S		L^*		a^*		b^*	
glass@epoxy	VL	UV	VL	UV	VL	UV	VL	UV
AEA_0	0.43	0.34	91.37	91.25	−2.53	−2.27	2.10	1.98
AEA_1	0.80	1.62	88.65	86.53	−2.31	−9.40	1.91	20.63
AEA_2	0.86	1.93	88.27	85.48	−2.27	−11.56	1.78	18.32
AEA_3	0.90	2.27	87.71	84.53	−2.11	−15.02	1.72	16.20
AEA_4	1.02	2.49	87.49	81.05	−1.97	−19.38	1.56	13.20
AEA_5	1.08	2.82	87.09	78.34	−1.93	−22.80	1.44	8.05
AEA_6	1.15	3.06	86.70	76.92	−1.70	−24.63	1.24	5.46
AEA_7	1.50	3.57	86.35	73.20	−1.51	−26.65	1.10	3.04
AEA_8	1.96	3.88	85.97	72.60	−1.43	−27.34	0.85	2.52

state, indicating fluorescence emission. On the other hand, turning off the UV lamp showed that the luminous glass@epoxy substrates with higher amounts of phosphor nanoparticles (AEA_3 and AEA_8) slowly returned to their transparent state, indicating afterglow emission. As the concentration of phosphor nanoparticles in the samples was increased from AEA_1 to AEA_8, the $+b^*$ values dropped, while the $-a^*$ values increased. Both AEA_7 and AEA_8 glass@epoxy substrates with the higher phosphor concentrations displayed a white color. It follows that the AEA_2 glass@epoxy sample, although appearing colorless under visible light, had the highest levels of photoinduced greener fluorescence and photochromic activity, while the long-lasting luminous AEA_6 glass@epoxy sample kept its colorless appearance with the highest phosphorescent greenish emission.[48−53]

3.6. Hydrophobicity and UV-Shielding. The contact angle increased from 141.3° for the blank sample (AEA_0) to 145.7° when the AEANP content was added to the glass@epoxy hybride (AEA_1). Subsequently, when the phosphor ratio increased from AEA_1 to AEA_6, a roughened surface was created by the AEA nano-scaled particles to result in improved contact angle from 145.7 to 154.6°. Further increasing the concentration of AEA nanoparticles caused lower spaces between the nanoparticles, which slightly decrease the roughness and contact angle of AEA_7 and AEA_8. Protecting against sun damage, erythema, and skin cancer is much easier with the use of smart windows that can block UV radiation.[25,27] The UV-blocking capabilities of the glowing glass@epoxy substrates were evaluated, as shown in Table 4. Strong UV protection was detected in the photoluminescent glass@epoxy substrates owing to the immobilized phosphor in AEA_1, which has a high UV absorption capability. Therefore, AEA_1 greatly outperformed AEA_0 in terms of its ability to block the harmful UV rays. The ultraviolet blocking characteristics of the luminescent colorless glass@epoxy hybrids were also enhanced by an increase in the AEANP concentration. The glowing transparent glass@epoxy hybrid can be utilized as a smart window with an energy-saving characteristic. The photochromic window receives a considerable amount of UV light during the daytime. Thus, it produces a greenish color that decreases the exposure of the interior rooms to sunlight by up to 86%. When the sunlight is weak, the photochromic glass@epoxy hybrid reverts to its colorless form to allow more light to go through inside the building rooms.

Table 4. Contact Angles and UPF of the Prepared Glass@epoxy Substrates

glass@epoxy	contact angle (°)	UPF
AEA_0	141.3	32
AEA_1	145.7	57
AEA_2	146.0	74
AEA_3	148.5	90
AEA_4	152.6	133
AEA_5	153.4	177
AEA_6	154.6	195
AEA_7	154.1	240
AEA_8	153.9	269

3.7. Mechanical Screening. The glass@epoxy durability can be drastically improved when immobilized with nanoparticles.[41−46] The focus of the current research was to prepare a transparent glass@epoxy with a smooth surface. Thus, tensile and scratch tests were conducted to assess the glass@epoxy mechanical characteristics. The scratching resistance was measured by a scratching pencil as a simple and efficient approach.[42] Scratch patterns were made on the glass@epoxy hybrid composites by scratch pencils (6B to 9H). The HB pencil hardness was sufficient to scratch the AEANP-free glass@epoxy sample (AEA_0). From AEA_1 to AEA_8, the luminous glass@epoxy substrates demonstrated scratch resistance of up to F, H, H, 2H, 2H, 2H, 3H, and 3H, respectively. It was found that increasing the phosphor concentration enhanced the glass@epoxy scratch resistance. Figure 7 depicts that the tensile strength of glass@epoxy was explored against the AEANP ratio. It was increased with the increase in AEANP ratio. The AEANPs, which are excellent stress transmitting agents in the glass@epoxy structure, are responsible for the increased tensile strength. As the AEANP ratio increased, so did the tensile strength of the glass@epoxy hybrid. The tensile

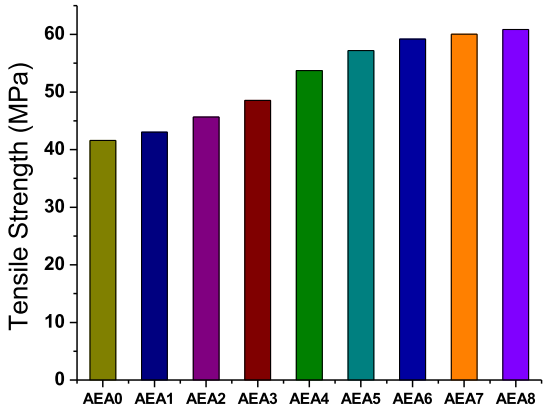

Figure 7. Tensile strength of glass@epoxy against AEANP content.

https://doi.org/10.1021/acsomega.2c07554
ACS Omega 2023, 8, 1683−1692

strength of an epoxy is enhanced by increasing the phosphor ratio due to the formation of stronger intermolecular coordinative bonds between epoxy oxygen and Al(III) in the AEA structure. Aluminum acts as a coordinate cross-linker between oxygen atoms on the epoxy polymer chains, causing the phosphor to create the 3D polymer network of greater molecular weight.[35]

4. CONCLUSIONS

The current study focused on the development of UV-responsive smart windows by loading AEANPs onto a glass@epoxy hybrid host material. Smart window technology can be built using these glass@epoxy substrates because of their photochromic and long-lasting luminescence features. The present method can be used to create colorless glass@epoxy hybrid nanocomposites with color-shifting capabilities and photochromic-reliant switching light transmittance. This straightforward method demonstrated the feasibility of creating photochromic glass@epoxy substrates with desirable properties such as transparency, photostability, UV protection, and hydrophobicity. The TEM measurements showed that the diameters of the produced phosphor nanoparticles are in the 43−98 nm range. Multifunctional photoluminescent transparent glass@epoxy substrates were prepared using a straightforward electrospinning process, in which glass nanofibers and AEANPs were homogeneously embedded. In this study, EDX, SEM, and XRF were used to analyze the morphological characteristics of the glass@epoxy substrates. Luminescent spectra and CIE Lab parameters indicated that the glass@epoxy substrates with luminescent qualities exhibited photochromic behavior, changing color from transparent to greenish under UV light. The contact angle of the luminous glass@epoxy hybrid nanocomposites showed that the hydrophobicity increases from 141.3 to 154.6° when the phosphor ratio increases. Increases in the phosphor ratio were also shown to boost scratch resistance and tensile strength. The ideal ratio for fluorescence photochromism in glass@epoxy was reported to be 1%, resulting in transparent glass@epoxy with the brightest green emission under UV light. The best ratio for long-lasting phosphorescence under UV light was reported to be 6% for the colorless glass@epoxy with the strongest phosphorescent green emission. The luminous glass@epoxy hybrid composites have showed a high photostability.

AUTHOR INFORMATION

Corresponding Authors

Nashwa M. El-Metwaly − *Department of Chemistry, Faculty of Applied Sciences, Umm Al-Qura University, Makkah 24382, Saudi Arabia;* orcid.org/0000-0002-0619-6206; Email: rania.zaky@yahoo.com

Rania Zaky − *Department of Chemistry, Faculty of Science, Mansoura University, Mansoura 35516, Egypt*; Email: n_elmetwaly00@yahoo.com, nmmohamed@uqu.edu.sa

Authors

Amal T. Mogharbel − *Department of Chemistry, Faculty of Science, University of Tabuk, Tabuk 71474, Saudi Arabia*

Ahmad A. Alluhaybi − *Department of Chemistry, College of Sciences & Arts, King Abdulaziz University, Rabigh 21589, Saudi Arabia*

Awatif R. Z. Almotairy − *Department of Chemistry, Faculty of Science, Taibah University, Yanbu 30799, Saudi Arabia*

Meshari M. Aljohani − *Department of Chemistry, Faculty of Science, University of Tabuk, Tabuk 71474, Saudi Arabia*

Complete contact information is available at: https://pubs.acs.org/10.1021/acsomega.2c07554

Notes

The authors declare no competing financial interest.

Consent to publish: the author(s) agree to publish the article under the Creative Commons Attribution License.

Availability of data and materials: all data generated or analyzed during this study are included in this published article.

ACKNOWLEDGMENTS

The authors would like to thank the Deanship of Scientific Research at Umm Al-Qura University for supporting this work by grant code: (22UQU4350527DSR04).

REFERENCES

(1) Hu, R.; Zhang, Y.; Zhao, Y.; Wang, X.; Li, G.; Wang, C. UV−Vis-NIR broadband-photostimulated luminescence of LiTaO3: Bi3+ long-persistent phosphor and the optical storage properties. *Chem. Eng. J.* **2020**, *392*, 124807.

(2) Yang, Y.-M.; Li, Z. Y.; Zhang, J. Y.; Lu, Y.; Guo, S. Q.; Zhao, Q.; Wang, X.; Yong, Z. J.; Li, H.; Ma, J. P.; Kuroiwa, Y. X-ray-activated long persistent phosphors featuring strong UVC afterglow emissions. *Light Sci. Appl.* **2018**, *7*, 88.

(3) Wang, C.; Jin, Y.; Lv, Y.; Ju, G.; Liu, D.; Chen, L.; Li, Z.; Hu, Y. Trap distribution tailoring guided design of super-long-persistent phosphor Ba 2 SiO 4: Eu 2+, Ho 3+ and photostimulable luminescence for optical information storage. *J. Mater. Chem. C* **2018**, *6*, 6058−6067.

(4) El-Newehy, M. H.; Kim, H. Y.; Khattab, T. A.; El-Naggar, M. E. Development of highly photoluminescent electrospun nanofibers for dual-mode secure authentication. *Ceram. Int.* **2022**, *48*, 3495−3503.

(5) Xiong, P.; Peng, M. Recent advances in ultraviolet persistent phosphors. *Opt. Mater.: X* **2019**, *2*, 100022.

(6) Zhou, Z.; Li, Y.; Peng, M. Near-infrared persistent phosphors: Synthesis, design, and applications. *Chem. Eng. J.* **2020**, *399*, 125688.

(7) Cai, H.; Song, Z.; Liu, Q. Infrared-photostimulable and long-persistent ultraviolet-emitting phosphor LiLuGeO 4: Bi 3+, Yb 3+ for biophotonic applications. *Mater. Chem. Front.* **2021**, *5*, 1468−1476.

(8) El-Newehy, M. H.; Kim, H. Y.; Khattab, T. A.; El-Naggar, M. E. Production of photoluminescent transparent poly (methyl methacrylate) for smart windows. *Luminescence* **2022**, *37*, 97−107.

(9) Al-Qahtani, S. D.; Alkhamis, K.; Alfi, A. A.; Alhasani, M.; El-Morsy, M. H.; Sedayo, A. A.; El-Metwaly, N. M. Simple Preparation of Multifunctional Luminescent Textile for Smart Packaging. *ACS Omega* **2022**, *7*, 19454−19464.

(10) Huang, K.; Le, N.; Wang, J. S.; Huang, L.; Zeng, L.; Xu, W. C.; Li, Z.; Li, Y.; Han, G. Designing next generation of persistent luminescence: recent advances in uniform persistent luminescence nanoparticles. *Adv. Mater.* **2022**, *34*, 2107962.

(11) Wu, S.; Li, Y.; Ding, W.; Xu, L.; Ma, Y.; Zhang, L. Recent advances of persistent luminescence nanoparticles in bioapplications. *Nano-Micro Lett.* **2020**, *12*, 70.

(12) Zhu, Q.; Xiahou, J.; Li, X.; Sun, X.; Li, J. G. Defect cluster engineering in ZnGa2− x (Mg/Ge) x O4: Cr3+ nanoparticles for remarkably improved NIR persistent luminescence. *J. Am. Ceram. Soc.* **2021**, *104*, 4594−4605.

(13) Wang, J. X.; Li, C.; Tian, H. Energy manipulation and metal-assisted photochromism in photochromic metal complex. *Coord. Chem. Rev.* **2021**, *427*, 213579.

(14) Zhao, J. L.; Li, M. H.; Cheng, Y. M.; Zhao, X. W.; Xu, Y.; Cao, Z. Y.; You, M. H.; Lin, M. J. Photochromic crystalline hybrid materials with switchable properties: Recent advances and potential applications. *Coord. Chem. Rev.* **2023**, *475*, 214918.
(15) Gulati, G. K.; Gulati, L. K.; Kumar, S. Recent progress in multi-stimulable photochromic oxazines with their wide-ranging applications. *Dyes Pigm.* **2021**, *192*, 109445.
(16) Wakayama, Y.; Hayakawa, R.; Higashiguchi, K.; Matsuda, K. Photochromism for optically functionalized organic field-effect transistors: A comprehensive review. *J. Mater. Chem. C* **2020**, *8*, 10956−10974.
(17) Han, S. D.; Hu, J. X.; Wang, G. M. Recent advances in crystalline hybrid photochromic materials driven by electron transfer. *Coord. Chem. Rev.* **2022**, *452*, 214304.
(18) Kayani, A. B.; Kuriakose, S.; Monshipouri, M.; Khalid, F. A.; Walia, S.; Sriram, S.; Bhaskaran, M. UV photochromism in transition metal oxides and hybrid materials. *Small* **2021**, *17*, 2100621.
(19) Yuan, J.; Yuan, Y.; Tian, X.; Wang, H.; Liu, Y.; Feng, R. Photoswitchable boronic acid derived salicylidenehydrazone enabled by photochromic spirooxazine and fulgide moieties: Multiple responses of optical absorption, fluorescence emission, and quadratic nonlinear optics. *J. Phys. Chem. C* **2019**, *123*, 29838−29855.
(20) Fedorov, Y. V.; Shepel, N. E.; Peregudov, A. S.; Fedorova, O. A.; Deligeorgiev, T.; Minkovska, S. Modulation of photochromic properties of spirooxazine bearing sulfobutyl substituent by metal ions. *J. Photochem. Photobiol., A* **2019**, *371*, 453−460.
(21) Khattab, T. A.; Tolba, E.; Gaffer, H.; Kamel, S. Development of electrospun nanofibrous-walled tubes for potential production of photoluminescent endoscopes. *Ind. Eng. Chem. Res.* **2021**, *60*, 10044−10055.
(22) Chandrakar, P.; Baghel, R. N.; Bisen, D. P.; Chandra, B. P. Persistent luminescence of CaMgSi2O6: Eu2+, Dy3+ and CaMgSi2O6: Eu2+, Ce3+ phosphors prepared using the solid-state reaction method. *Luminescence* **2016**, *31*, 164−167.
(23) Delgado, T.; Afshani, J.; Hagemann, H. Spectroscopic study of a single crystal of SrAl2O4: Eu2+: Dy3+. *J. Phys. Chem. C* **2019**, *123*, 8607−8613.
(24) Cui, C.; Jiang, G.; Huang, P.; Wang, L.; Liu, D. Effect of Eu3+ concentration on the luminescence properties of Y2O2S: Eu3+, Mg2+, Ti4+ nanotubes. *Ceram. Int.* **2014**, *40*, 4725−4730.
(25) Al-Qahtani, S. D.; Alzahrani, S. O.; Snari, R. M.; Al-Ahmed, Z. A.; Alkhamis, K.; Alhasani, M.; El-Metwaly, N. M. Preparation of photoluminescent and photochromic smart glass window using sol-gel technique and lanthanides-activated aluminate phosphor. *Ceram. Int.* **2022**, *48*, 17489−17498.
(26) Elsawy, H.; Sedky, A.; Abou Taleb, M. F.; El-Newehy, M. H. Colour-switchable and photoluminescent polyvinyl chloride for multifunctional smart applications. *Luminescence* **2022**, *37*, 1504−1513.
(27) Al-Qahtani, S.; Aljuhani, E.; Felaly, R.; Alkhamis, K.; Alkabli, J.; Munshi, A.; El-Metwaly, N. Development of photoluminescent translucent wood toward photochromic smart window applications. *Ind. Eng. Chem. Res.* **2021**, *60*, 8340−8350.
(28) Hassabo, A. G.; Mohamed, A. L.; Khattab, T. A. Preparation of cellulose-based electrospun fluorescent nanofibres doped with perylene encapsulated in silica nanoparticles for potential flexible electronics. *Luminescence* **2022**, *37*, 21−27.
(29) Walfort, B.; Gartmann, N.; Afshani, J.; Rosspeintner, A.; Hagemann, H. Effect of excitation wavelength (blue vs near UV) and dopant concentrations on afterglow and fast decay of persistent phosphor SrAl2O4: Eu2+, Dy3+. *J. Rare Earths* **2022**, *40*, 1022−1028.
(30) Saatchi, A.; Arani, A. R.; Moghanian, A.; Mozafari, M. Synthesis and characterization of electrospun cerium-doped bioactive glass/chitosan/polyethylene oxide composite scaffolds for tissue engineering applications. *Ceram. Int.* **2021**, *47*, 260−271.
(31) Wen, S.; Liu, L.; Zhang, L.; Chen, Q.; Zhang, L.; Fong, H. Hierarchical electrospun SiO2 nanofibers containing SiO2 nanoparticles with controllable surface-roughness and/or porosity. *Mater. Lett.* **2010**, *64*, 1517−1520.
(32) Chen, Q.; Zhang, L.; Yoon, M. K.; Wu, X. F.; Arefin, R. H.; Fong, H. Preparation and evaluation of nano-epoxy composite resins containing electrospun glass nanofibers. *J. Appl. Polym. Sci.* **2012**, *124*, 444−451.
(33) Abumelha, H. M. Simple production of photoluminescent polyester coating using lanthanide-doped pigment. *Luminescence* **2021**, *36*, 1024−1031.
(34) Abou-Melha, K. Preparation of photoluminescent nanocomposite ink toward dual-mode secure anti-counterfeiting stamps. *Arab. J. Chem.* **2022**, *15*, 103604.
(35) Ahmed, E.; Maamoun, D.; Hassan, T. M.; Khattab, T. A. Development of functional glow-in-the-dark photoluminescence linen fabrics with ultraviolet sensing and shielding. *Luminescence* **2022**, *37*, 1376−1386.
(36) Al-Qahtani, S. D.; Al-nami, S. Y.; Alkhamis, K.; Al-Ahmed, Z. A.; Binyaseen, A. M.; Khalifa, M. E.; El-Metwaly, N. M. Simple preparation of long-persistent luminescent paint with superhydrophobic anticorrosion efficiency from cellulose nanocrystals and an acrylic emulsion. *Ceram. Int.* **2022**, *48*, 6363−6371.
(37) Xue, J.; Wang, X.; Jeong, J. H.; Yan, X. Fabrication, photoluminescence and applications of quantum dots embedded glass ceramics. *Chem. Eng. J.* **2020**, *383*, 123082.
(38) Huang, X.; Guo, Q.; Kang, S.; Ouyang, T.; Chen, Q.; Liu, X.; Xia, Z.; Yang, Z.; Zhang, Q.; Qiu, J.; Dong, G. Three-dimensional laser-assisted patterning of blue-emissive metal halide perovskite nanocrystals inside a glass with switchable photoluminescence. *ACS Nano* **2020**, *14*, 3150−3158.
(39) Laia, C. A.; Ruivo, A. Photoluminescent glasses and their applications. *Fluorescence in Industry*; Springer, 2019; pp 365−388.
(40) Noh, H.; Kung, C. W.; Islamoglu, T.; Peters, A. W.; Liao, Y.; Li, P.; Garibay, S. J.; Zhang, X.; DeStefano, M. R.; Hupp, J. T.; Farha, O. K. Room temperature synthesis of an 8-connected Zr-based metal−organic framework for top-down nanoparticle encapsulation. *Chem. Mater.* **2018**, *30*, 2193−2197.
(41) Neukäufer, J.; Seyfang, B.; Grützner, T. Investigation of contact angles and surface morphology of 3D-printed materials. *Ind. Eng. Chem. Res.* **2020**, *59*, 6761−6766.
(42) Domene-López, D.; García-Quesada, J. C.; Martín-Gullón, I. A correlation between the Wolf-Wilburn scale and atomic force microscopy for anti-scratch resistance determination. *Prog. Org. Coat.* **2018**, *125*, 325−330.
(43) Jung, S.; Cho, D. Effect of fiber feeding route upon extrusion process on the electromagnetic, mechanical, and thermal properties of nickel-coated carbon fiber/polypropylene composites. *Composites, Part B* **2020**, *187*, 107861.
(44) Li, G. P.; Cao, F.; Zhang, K.; Hou, L.; Gao, R. C.; Zhang, W. Y.; Wang, Y. Y. Design of Anti-UV Radiation Textiles with Self-Assembled Metal−Organic Framework Coating. *Adv. Mater. Interfaces* **2020**, *7*, 1901525.
(45) Zheng, L.; Xiong, T.; Shah, K. W. Transparent nanomaterial-based solar cool coatings: Synthesis, morphologies and applications. *Sol. Energy* **2019**, *193*, 837−858.
(46) Ahmed, N.; Ahmed, R.; Rafiqe, M.; Baig, M. A. A comparative study of Cu−Ni alloy using LIBS, LA-TOF, EDX, and XRF. *Laser Part. Beams* **2017**, *35*, 1−9.
(47) El-Newehy, M. H.; Kim, H. Y.; Khattab, T. A.; Moydeen A, M.; El-Naggar, M. E. Synthesis of lanthanide-doped strontium aluminate nanoparticles encapsulated in polyacrylonitrile nanofibres: photoluminescence properties for anticounterfeiting applications. *Luminescence* **2022**, *37*, 40−50.
(48) Zheng, K.; Boccaccini, A. R. Sol-gel processing of bioactive glass nanoparticles: A review. *Adv. Colloid Interface Sci.* **2017**, *249*, 363−373.
(49) Alfattani, R.; Hassan, M. K.; Samy, A. M.; Ameer, A. K. Enhancing the Epoxy Flooring Materials to Avoid Dangerous of Electrostatic Charge and Slip Accidents. *Solid State Technol.* **2020**, *63*, 7756−7771.

https://doi.org/10.1021/acsomega.2c07554
ACS Omega 2023, 8, 1683−1692

(50) Mirza, F. A.; Soroushian, P. Effects of alkali-resistant glass fiber reinforcement on crack and temperature resistance of lightweight concrete. *Cem. Concr. Compos.* **2002**, *24*, 223−227.
(51) Hameed, A. M. Synthesis of Si/Cu amorphous adsorbent for efficient removal of methylene blue dye from aqueous media. J. Inorg. Organomet. *J. Inorg. Organomet. Polym. Mater.* **2020**, *30*, 2881−2889.
(52) Hamouda, I. M.; Beyari, M. M. Addition of glass fibers and titanium dioxide nanoparticles to the acrylic resin denture base material: comparative study with the conventional and high impact types. *Oral Health Dent. Manag.* **2014**, *13*, 107−112.
(53) Mustakim, S. M.; Das, S. K.; Mishra, J.; Aftab, A.; Alomayri, T. S.; Assaedi, H. S.; Kaze, C. R. Improvement in fresh, mechanical and microstructural properties of fly ash-blast furnace slag based geopolymer concrete by addition of nano and micro silica. *Silicon* **2021**, *13*, 2415−2428.

https://doi.org/10.1021/acsomega.2c07554
ACS Omega 2023, 8, 1683−1692